

Characterization of substrates for use in X-ray multilayer optics

G. S. Lodha,^{a,*†} K. Yamashita,^a K. Haga,^a
H. Kunieda,^a N. Nakajo,^a N. Nakamura,^a K. Tamura,^a
Y. Tawara,^a J. M. Bennett,^b J. Yu^c and Y. Namba^c

^aDepartment of Physics, Nagoya University, Furo-cho, Chikusa-ku, Nagoya 464-8602, Japan, ^bNaval Air Warfare Center, China Lake, California 93555, USA, and ^cDepartment of Mechanical Engineering, Chubu University, 1200 Matsumotocho, Kasugai, Aichi 487, Japan.
E-mail: lodha@satio.phys.nagoya-u.ac.jp

(Received 4 August 1997; accepted 14 January 1998)

The optical performance of platinum–carbon multilayers deposited onto different substrates has been examined. Specular reflectivity and non-specular diffuse scattering were measured to study the replication of substrate roughness into the multilayer structure. Surface topography was measured before and after deposition using a scanning probe microscope and a mechanical profiler.

Keywords: X-ray multilayers; X-ray reflectivity; diffuse scattering; scanning probe microscopes; surface roughness.

1. Introduction

There is a continued need in X-ray optics to fabricate multilayers with small period lengths. These multilayer structures are used for high-energy applications (10–100 keV) in astronomy, synchrotron radiation beamlines, and X-ray microscopy (Yamashita *et al.*, 1998). For these applications we need to deposit multilayers onto supersmooth surfaces with surface and interfacial roughness controlled over a broad range of spatial frequencies. In order to realize the full potential of multilayer X-ray optics, various types of substrates need to be characterized before and after coating with multilayer structures.

Several groups have reported interfacial roughness correlations to determine the correlated roughness propagating from the substrate into the multilayer structure by measuring diffuse scattering, mostly at Cu $K\alpha$ (8.047 keV) or near this energy (Jiang *et al.*, 1992; Kortright, 1991; Savage *et al.*, 1993; Spiller *et al.*, 1993; Vitta *et al.*, 1997). These groups have shown that if the interface roughness is vertically correlated, the diffuse scattered intensity is concentrated at angles near the Bragg maximum. Most of the above authors have not studied the interfacial roughness for well evaluated surfaces mapped by surface topographic techniques. Except for Jiang *et al.* (1992) and Spiller *et al.* (1993), the authors report on correlated roughness studies in X-ray multilayer structures using rocking-curve scans. In these scans the detector is fixed at an angle 2θ and the sample is rocked. The incident angle and scattering angle both change, and the scattered light can be influenced by interference between the incident and scattered fields which changes with the change in

† On leave from Centre for Advanced Technology, Indore 452013, India; e-mail: lodha@cat.cat.ernet.in; fax: +91 731 481525.

angles. Pt/C multilayers have been shown to be a good combination for soft and hard X-ray applications (Lodha *et al.*, 1994). We have performed detector scans on Pt/C multilayers deposited on different substrates, where the incident angle is fixed, so the field distribution inside the multilayer coating remains constant during the scan, and so the structure observed in the scattered light is only caused by phase superposition of the scattered beams.

For samples, we used an SiO₂ wafer produced for the microelectronics industry, a conventionally polished fused silica substrate, a gold-coated replica foil made for an X-ray telescope application (Tamura *et al.*, 1997), and a float glass microscope slide. X-ray specular reflectivity and diffuse scattering were measured using a precision X-ray reflectometer (Lodha *et al.*, 1998). With a 1 mm source size of a rotating-anode X-ray generator, the incident beam had an angular divergence of 20 arcsec at a distance of 10 m. Topographic surface maps were made in the dynamic force microscope mode using a scanning probe microscope (SPM) system built by Seiko Instruments Inc., Japan. Surface profiles were measured with a Rank Taylor Hobson Talystep mechanical profiler equipped with Bennett–Fellows software (Bennett & Mattsson, 1989). Multilayer coatings were deposited in a vacuum chamber using a DC magnetron source specially designed for coating the inner walls of cylindrical surfaces (Tamura *et al.*, 1997).

2. Results and discussion

Table 1 lists the roughness of four different substrates before and after deposition of Pt/C multilayers. Roughness values were obtained by fitting each measured X-ray reflectance curve with the profiles calculated by successive applications of the Fresnel equation at each interface with a Debye–Waller-like attenuation term, accounting for the reduction in scattered amplitude because of interfacial roughness. The discrepancy in roughness value for an SiO₂ wafer before coating is probably associated with the fabrication process of the wafer. The penetration depth calculated for fused silica at Al $K\alpha$ energy is 0.35 μm at an angle of incidence of 5°, while Cu $K\alpha$ penetrates 2.3 μm at a 1° angle of incidence. For multilayer coatings, the roughness calculated at Al $K\alpha$ and Cu $K\alpha$ energies were consistent. This was an indication of a constant roughness throughout the multilayer stack since the penetration depth at these two energies was different. As is clear from Table 1, the roughness values derived from X-ray specular reflection (XR) correlate well with the SPM and Talystep measurements.

Fig. 1 shows a 1 $\mu\text{m} \times 1 \mu\text{m}$ SPM topographic map of the SiO₂ wafer coated with a Pt/C multilayer, $N = 20$, $d = 42.5 \text{ \AA}$. For this supersmooth surface, the roughness after coating with the Pt/C multilayer as measured by the SPM and Talystep (1–2 \AA) is lower than the value of 3 \AA obtained by XR measurements at Al $K\alpha$, Cu $K\alpha$ and Mo $K\alpha$. The difference is probably because the roughness calculated from XR includes the interfacial roughness contribution. The lower roughness of 3.5 \AA after coating the replica foil, compared with the 5 \AA roughness measured before coating, is caused by a reduction in the scattering contribution at the Bragg peak from uncorrelated high-frequency roughness components by a factor proportional to the number of multilayer periods contributing to the X-ray reflection at the Bragg peak. A similar effect is seen for the fused silica sample. The high-frequency roughness on the surface is not picked up in SPM and

Table 1

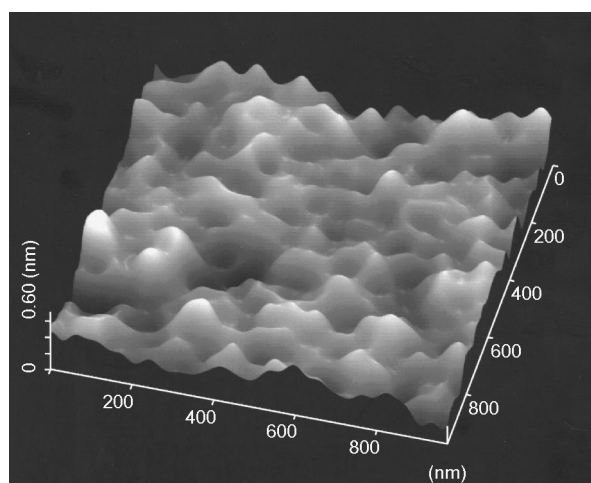
R.m.s. roughness of different substrates determined from X-ray specular reflection (XR) measurements, scanning probe microscope (SPM) topographic measurements and Talystep profile measurements before and after deposition of multilayers.

	Before deposition				After multilayer deposition					
	Al $K\alpha$	XR	Cu $K\alpha$	SPM 100 μm^2	Talystep 100 μm	Al $K\alpha$	XR	Cu $K\alpha$	SPM 100 μm^2	Talystep 100 μm
SiO ₂ wafer	0		5	0.67	1.37	3.0		3.0	1.05	1.92
Fused silica	8		–	4.02	6.52	4.5		5.5	6.59	7.16
Float glass	–		–	0.94	2.15	3.0		3.0	1.40	2.51
Replica foil	–		5	–	–	–		3.5	4.21	–

Talystep due to the finite radius of the measuring tip and limited sampled data points in the scanned area.

Fig. 2 shows a representative reflectivity curve measured at Cu $K\alpha$ (8.047 keV) along with the profile calculated from the model. This curve is for a Pt/C multilayer, $N = 30$, deposited on the replica foil substrate. Note the excellent agreement between the calculated and measured curves.

Fig. 3 shows detector scans (8.047 keV Cu $K\alpha$, 0.2 mm pinhole in the incident beam, fixed incident angle, 0.3 mm slit in front of the proportional counter which is 17 cm away from the sample rotation axis). Fig. 3(a) is for the fused silica sample coated with 20 layer pairs of Pt/C. The structural parameters, derived from the X-ray reflectivity measurements, are period length, $d = 50.6 \text{ \AA}$, ratio of platinum thickness to period thickness, $\Gamma = 0.57$, and r.m.s. roughness, $\sigma = 5.5 \text{ \AA}$. The solid curve with filled squares represents a detector scan with the incident angle fixed at the first Bragg peak position, $\theta_i = \theta_{b1} = 0.96^\circ$. The detector passes through the first Bragg peak at 1.92° (marked '1'). We observe increased scattering at a detector angle of 3.6° (marked '2'). This angle corresponds to the position of the second-order maximum in the reflectivity curve. This is caused by non-specular scattering from correlated rough interfaces, which peaks at the Bragg condition. The magnitude of scattering at these points depends on the degree of correlation. The dashed curve with open circles represents measurements with $\theta_i = 1.16^\circ$ (slightly larger than θ_{b1}). The first intensity maximum is split into two peaks marked 'a' and 'b'. Peak 'a' at 1.92° is caused by non-specular amorphous scattering at the first Bragg peak arising from correlated roughness in the multilayer structure. Peak 'b', which appears at $2\theta = 2.32^\circ = 2\theta_i$, is caused by specular reflection. The position and intensity of the peak marked '2' remains the same.

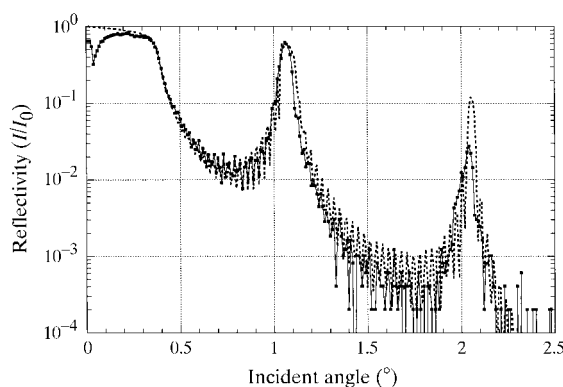
**Figure 1**

$1 \mu\text{m} \times 1 \mu\text{m}$ SPM topographic map of an SiO₂ wafer coated with a Pt/C multilayer, $N = 20$, $d = 42.5 \text{ \AA}$.

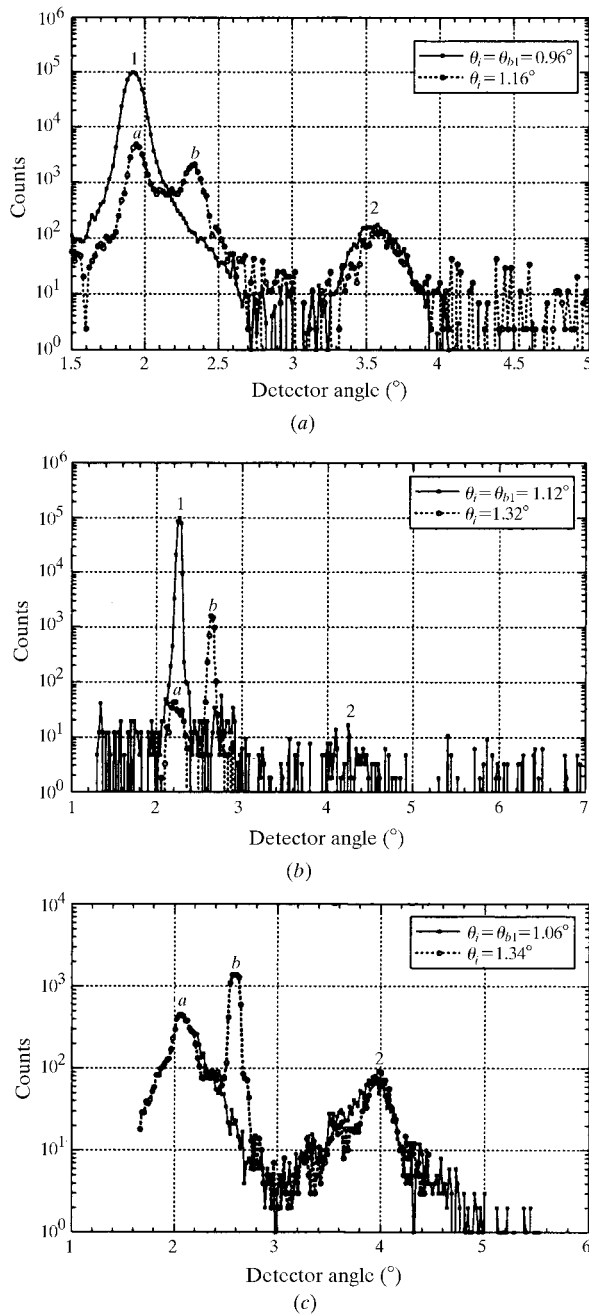
Figs. 3(b) and 3(c) show similar measurements for the SiO₂ wafer ($N = 20$, $d = 42.5 \text{ \AA}$, $\Gamma = 0.57$, $\sigma = 3 \text{ \AA}$) and replica foil ($N = 30$, $d = 43.7 \text{ \AA}$, $\Gamma = 0.35$, $\sigma = 3.5 \text{ \AA}$) substrates, respectively. Clearly, the scattering caused by correlated roughness is much lower for the SiO₂ wafer where the peak marked '2' is hardly visible and the intensity of the peak marked 'a' is also much lower. For the replica foil, the roughness calculated from the reflectivity is 3.5 \AA (Fig. 2) but Fig. 3(c) shows high scattering because of high correlated roughness. Thus, it is essential to calculate both the specular and diffuse components of the scattered radiation.

The correlated roughness scattering enhancement at positions of Bragg maxima are explained on the basis of standing-wave field enhanced coherent atomic scattering from amorphous layers having periodicity in the growth direction (Jiang *et al.*, 1992). With the increase in incident energy, coherent atomic scattering increases as the number of free electrons per atom increases. For this reason we made the same measurements at Mo $K\alpha$ (17.48 keV). For Mo $K\alpha$ measurements the first Bragg angle was near 0.5° , requiring a smaller incident beam size, smaller slit on the detector and a larger distance between sample and detector. Thus, for these scans we used a 0.15 mm slit in front of the CdZnTe detector which was 35 cm away from the sample. The beam size was defined by a 0.1 mm slit in the incident beam. Fig. 4 shows detector scans at two angles near the first Bragg peak for the SiO₂ wafer. Scattering at the second Bragg peak position, caused by correlated roughness, which was hardly visible at 8.047 keV (Fig. 3b), can be clearly seen at this higher energy, 17.48 keV.

In the present study, the observed interference in the scattered light measured by the detector scans has been used as an indication of correlated roughness between various substrates. We see that comparatively rough substrates, *e.g.* polished fused silica and replica foils, show a high degree of correlated roughness.

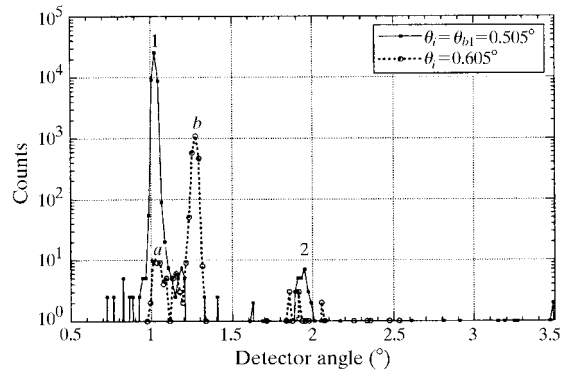
**Figure 2**

Representative reflectivity curve measured at Cu $K\alpha$ (8.047 keV) (squares and solid line) along with the calculated profile (short dashed line). This curve is for a Pt/C multilayer, $N = 30$, deposited on a replica foil substrate.

**Figure 3**

Intensity from detector scans at 8.047 keV ($\text{Cu } K\alpha$) for Pt/C multilayers coated on (a) a fused silica substrate, (b) a 2 mm-thick SiO_2 wafer and (c) a replica foil used for X-ray telescopes. Peaks marked '1' and '2' correspond to positions of Bragg maxima. Solid curves with filled squares are for the incident angle fixed at the first Bragg maxima. Dashed curves with open circles are with the incident angle fixed at 0.2° above the first Bragg maximum. These measurements were made with a proportional counter with a 0.3 mm slit and 0.2 mm-diameter incident beam.

High reflectivity at the Bragg peaks is an indication of low non-correlated roughness, but for X-ray imaging applications the roughness replication over a broad frequency band needs to be measured. SiO_2 wafers produced for the microelectronics industry would seem to be excellent inexpensive substrates for multilayer X-ray mirrors. They have very smooth surfaces and the correlated roughness is also low. However, the major drawback is that they are thin (normally less than 2 mm) and so generally

**Figure 4**

Intensity from detector scans measured at 17.48 keV ($\text{Mo } K\alpha$) for a Pt/C multilayer deposited on a 2 mm-thick SiO_2 wafer. The rest is the same as in Fig. 3 except that a CdZnTe solid-state detector with a 0.15 mm slit was used and the beam size was defined by a 0.1 mm slit in the incident beam.

have large figure errors. This figure error will not repeat from sample to sample. Replica foils are good light-weight substrates for multilayer deposition since they have low r.m.s. roughness and high peak reflectivity when coated with multilayers, but they are useful only for applications where imaging requirements are not very stringent. The 7 mm-thick fused silica sample was not a good substrate for multilayer deposition.

The above discussion is still qualitative in nature. For fitting the experimental data with theoretical models, a couple of simplified assumptions need to be made regarding the roughness distribution. This distribution may change depending on the initial starting substrate, number of layer pairs, material combination, method of deposition and model of thin film growth. So the numbers derived for correlated roughness are model dependent. We have not attempted to make a model fit of the experimental data. Instead we changed one parameter, the substrate type, to compare the relative contribution of the scattered intensity with the type of the substrate.

This work was supported in part by a Grant-in-Aid for Scientific Research on Specially Promoted Research, Contract No. 01702007, from the Ministry of Education, Science, Sports and Culture, Japan. GSL, JMB and JY were supported by grants from the Japan Society for the Promotion of Science.

References

- Bennett, J. M. & Mattsson, L. (1989). *Introduction to Surface Roughness and Scattering*, p. 20. Washington, DC: Optical Society of America.
- Jiang, X., Metzger, T. H. & Peisl, J. (1992). *Appl. Phys. Lett.* **61**, 904–906.
- Kortright, J. B. (1991). *J. Appl. Phys.* **70**, 3620–3625.
- Lodha, G. S., Yamashita, K., Kunieda, H., Tawara, Y., Yu, J., Namba, Y. & Bennett, J. M. (1998). *Appl. Opt.* To be published.
- Lodha, G. S., Yamashita, K., Suzuki, T., Hatsukade, I., Tamura, K., Ishigami, T., Takahama, S. & Namba, Y. (1994). *Appl. Opt.* **33**, 5869–5874.
- Savage, D. E., Phang, Y.-H., Rownd, J. J., MacKay, J. F. & Lagally, M. G. (1993). *J. Appl. Phys.* **74**, 6158–6164.
- Spiller, E., Stearns, D. & Krumrey, M. (1993). *J. Appl. Phys.* **74**, 107–118.
- Tamura, Y., Yamashita, K., Kunieda, H., Tawara, K., Furuzawa, A., Haga, K., Lodha, G. S., Nakajo, N., Nakamura, N., Okajima, T., Tsuda, O., Serlemitsos, P. J., Tueller, J., Petre, R., Ogasaka, Y., Soong, Y. & Chan K. (1997). *Proc. SPIE*, **3113**, 285–292.
- Vitta, S., Metzger, T. H. & Peisi, J. (1997). *Appl. Opt.* **36**, 1472–1481.
- Yamashita, K., Akiyama, K., Haga, K., Kunieda, H., Lodha, G. S., Nakajo, N., Nakamura, N., Okajima, T., Tamura, K. & Tawara, Y. (1998). *J. Synchrotron Rad.* **5**, 711–713.